Youlee Lee[1]*
Jong Min Lee[2]*
Pan-Kee Bae[3]
Il Yup Chung[1,4]
Bong Hyun Chung[3]**
Bong Geun Chung[2]

[1]Department of Bionano Technology, Hanyang University, Ansan, Korea
[2]Department of Mechanical Engineering, Sogang University, Seoul, Korea
[3]BioNano Heath Guard Research Center, Korea Research Institute of Bioscience and Biotechnology, Daejeon, Korea
[4]Department of Molecular and Life Science, Hanyang University, Ansan, Korea

Received October 3, 2014
Revised December 20, 2014
Accepted January 14, 2015

Research Article

Photo-crosslinkable hydrogel-based 3D microfluidic culture device

We developed the photo-crosslinkable hydrogel-based 3D microfluidic device to culture neural stem cells (NSCs) and tumors. The photo-crosslinkable gelatin methacrylate (GelMA) polymer was used as a physical barrier in the microfluidic device and collagen type I gel was employed to culture NSCs in a 3D manner. We demonstrated that the pore size was inversely proportional to concentrations of GelMA hydrogels, showing the pore sizes of 5 and 25 w/v% GelMA hydrogels were 34 and 4 μm, respectively. It also revealed that the morphology of pores in 5 w/v% GelMA hydrogels was elliptical shape, whereas we observed circular-shaped pores in 25 w/v% GelMA hydrogels. To culture NSCs and tumors in the 3D microfluidic device, we investigated the molecular diffusion properties across GelMA hydrogels, indicating that 25 w/v% GelMA hydrogels inhibited the molecular diffusion for 6 days in the 3D microfluidic device. In contrast, the chemicals were diffused in 5 w/v% GelMA hydrogels. Finally, we cultured NSCs and tumors in the hydrogel-based 3D microfluidic device, showing that 53–75% NSCs differentiated into neurons, while tumors were cultured in the collagen gels. Therefore, this photo-crosslinkable hydrogel-based 3D microfluidic culture device could be a potentially powerful tool for regenerative tissue engineering applications.

Keywords:
Hydrogel / Microfluidic device / Stem cell

DOI 10.1002/elps.201400465

1 Introduction

Neural stem cells (NSCs) are of great important cell sources for studying the neurodegenerative metabolic disease and spinal cord injury [1]. It has been known that NSCs give rise to differentiate into three major cell lineages, such as neurons, astrocytes, and oligodendrocytes [2]. In general, NSCs first differentiate into neurons, following by astrocytes and oligodendrocytes [3]. NSCs-derived neuronal differentiation has previously been investigated using extracellular matrix (ECM)-based hydrogels. For instance, NSCs isolated from embryonic cortical neuroepithelium were suspended with collagen type I gels to manipulate neuronal circuit in a 3D manner [4]. It showed that NSCs encapsulated within collagen gels gave rise to neurons. In contrast, glial fibrillary acidic protein-positive astrocytes and O4-positive oligodendrocytes were not observed until 10 days. Electrophysiology analysis showed that voltage-gated K^+ and Na^+ ion currents were altered when NSCs differentiated into Tuj1-positive neurons. However, it represented that the voltage-gated Na^+ ion current was not largely observed in undifferentiated NSCs. It also observed that NSC-derived neurons encapsulated inside collagen gels showed the synaptic vesicle recycling. Furthermore, 3D collagen type I gel-hyaluronan matrix has previously employed to induce NSC-derived neuronal differentiation [5]. It showed that the progenitor cells derived from embryonic brains were rapidly grown. NSCs cultured for 6 days in the 3D collagen type I gel-hyaluronan matrix largely gave rise to neurons (~70%). In contrast, 14% NSC-derived neurons were only observed at sixth day on the fibronectin-coated glass. It demonstrated that a large number of βIII-tubulin-positive cells showed mature neuronal differentiation, confirmed by expression of glutamate, γ-aminobutyric acid, and synapsin I.

Hydrogels are of great interest in applications for implantable materials and regenerative tissues. Hydrogels containing water contents hold complex polymeric chain structures in a 3D manner [6, 7]. In particular, hydrogels (e.g. gelatin, collagen, and hyaluronate) made from natural sources have widely been used as alternative materials to replace the tissue scaffold because the chemical and mechanical properties of biodegradable hydrogels are similar to properties of human tissues [8–10]. The hydrogel-based

Correspondence: Professor Bong Geun Chung, Department of Mechanical Engineering, Sogang University, Seoul, Korea, 121-742
E-mail: bchung@sogang.ac.kr

Abbreviations: ECM, extracellular matrix; **GelMA**, gelatin methacrylate; **MAP2**, microtubule-associated protein2; **NSC**, neural stem cell; **SEM**, scanning electron microscope

*These authors contributed equally to this work.
**Additional corresponding author: Dr. Bong Hyun Chung
E-mail: chungbh@kribb.re.kr

Colour Online: See the article online to view Figs. 1 and 4–7 in colour.

3D culture methods have widely been used for stem cell-based tissue engineering applications [11, 12]. In particular, photo-crosslinkable hydrogels have recently been used to regulate stem cell differentiation. For instance, copper-free click chemistry-based cytocompatible hydrogels have been used for the cell encapsulation and patterning in a spatial manner [13]. It showed that cell-encapsulated hydrogels were generated from poly(ethylene glycol) tetra-azide and self-quenched collagenase-sensitive detection peptide using a bis(cyclooctyne)-functionalized peptide crosslinker. It observed that fibroblast cells were spatially patterned within hydrogels containing Arg-Gly-Asp (RGD) peptides. This method could be useful for photo-sensitive fabrication of biologically functionalized hydrogels. The porous photo-crosslinkable methacrylamide chitosan has been used to induce NSC differentiation [14]. To regulate the porosity, D-mannitol crystals were mixed with methacrylamide chitosan. It showed that D-mannitol crystals enabled the increase of average pore sizes, resulting in increasing the oxygen diffusion rate. The growth of NSCs cultured with porous methacrylamide chitosan was inversely proportional to the porosity. In contrast, the porous methacrylamide chitosan scaffolds induced NSC differentiation. The methacrylate-modified hyaluronic acid–based hydrogels have previously used to regulate neural progenitor cell differentiation [15]. It investigated the effect of methacrylate-modified hyaluronic acid–based hydrogel concentrations on compressive moduli, showing that compressive moduli were increased with hydrogel concentrations. The neural progenitor cells were photo-encapsulated within hyaluronic acid hydrogels for neuronal differentiation. Interestingly, neural progenitor cells cultured with stiffer hydrogels largely differentiated into glial fibrillary acidic protein-positive astrocytes. It confirmed that the differentiation of neural progenitor cells was significantly affected by hydrogel mechanical properties. The photo-crosslinked RGD-alginate gels have also been used to direct adipose progenitor cells [16]. The mechanical properties of hydrogels were regulated by adhesion peptide density and Ca^{2+} concentration. The cells in stiffer hydrogels were more proliferated than those in compliant hydrogels and preadipocyte cells cultured within stiff hydrogels largely secreted vascular endothelial growth factors. It demonstrated that the adipose-derived differentiation was constrained by the mechanical rigidity of the hydrogel matrix.

The differentiation of stem cells is significantly affected by various extracellular microenvironments [17]. To manipulate stem cell fate, various multifunctional microfluidic devices have recently been developed [18–22]. For instance, compartmental microfluidic culture device has been developed to induce neuronal differentiation from murine embryonic stem cells [23]. Embryoid bodies-loaded into microfluidic culture device were differentiated into neurons and their axons extended through bridge microchannels, resulting in forming alignment of axons. The use of the 3D gel matrix as a scaffold is of significant benefit over traditional 2D cultures because it can mimic in vivo tissue environment. NSCs have previously been cultured in ECM-based 3D microfluidic devices [20]. NSCs and ECM hydrogels (e.g. collagen type I, Matrigel, and mixture of collagen I and Matrigel) loaded into the center of the microchannels, while growth medium containing various growth factors was placed on side channels. It investigated the effect of three ECM hydrogels on NSC differentiation in the microfluidic device. The quantitative real-time PCR analysis showed that NSCs cultured in 3D Matrigel-based hydrogels highly differentiated into neurons and oligodendrocytes compared to those in collagen gels because the laminin was the major ingredient of Matrigel. In contrast, quantitative real-time PCR analysis indicated that NSCs cultured in 3D ECM hydrogels containing Matrigel or collagen were not largely differentiated into astrocytes. Furthermore, 3D microfluidic device has been employed for culture of mouse embryonic stem cells, breast cancer cells, and hepatocytes [24]. The two-layer compartmentalized microfluidic device embedding semiporous membranes were used to pattern Janus culture of 3D spheroids. The heterogeneous spheroids were patterned in microfluidic hydrodynamic device and the shape of dynamic cellular micropatterning was regulated by the geometry of microchannels. It demonstrated that mouse embryonic stem cells were located on the inside of cell spheroids, whereas breast cancer cells (MDA-MB-231) or hepatocarcinoma cells (HepG2) were placed on outside of spheroids, suggesting that the Janus 3D cell spheroids could enable the control of spatial differentiation on mouse embryonic stem cells. Although previous 3D microfluidic devices were used for stem cell-based neuronal differentiation, they did not consider the effect of photo-crosslinkable hydrogels on molecular diffusions. In this paper, we develop photo-crosslinkable hydrogel-based 3D microfluidic device, consisting of five microchambers and four bridge microchannels, for culture of NSCs and tumors. We demonstrated that 25 w/v% photo-crosslinkable gelatin methacrylate (GelMA) hydrogels prevented the molecular diffusion from microchannels and NSCs encapsulated within the collagen type I gel-loaded microchamber differentiated into Tuj1- or microtubule-associated protein2 (MAP2)-positive neurons.

2 Materials and methods

2.1 Fabrication of 3D microfluidic culture device

The microchambers and bridge microchannels were fabricated by two-step photolithography methods as previously described [25]. To fabricate 3D microfluidic culture device, microchambers and bridge microchannels were designed by AutoCAD program. To fabricate bridge microchannels, SU-8 25 photoresist was spin-coated on a silicon wafer (1000 rpm, 60 s, and 40 μm in thickness). To fabricate microchambers, SU-8 100 was subsequently spin-coated on SU-8 25 photoresist-patterned substrates (1000 rpm, 60 s, and 250 μm in thickness). After development, PDMS precursor solution was molded from the photoresist-patterned silicon wafer and PDMS-based 3D microfluidic culture device was bonded into glass slides using oxygen plasma treatment (Femto Science, Korea).

2.2 GelMA hydrogel synthesis

The photo-crosslinkable GelMA hydrogels were synthesized as previously described [26, 27]. Briefly, type A porcine skin gelatin was stirred at 50°C and PBS (GIBCO, USA) was mixed until fully dissolved. Methacrylic anhydride was added with 0.5 mL/min rate under stirred conditions for 2 h. The mixture was dialyzed against distilled water using 12–14 kDa cutoff dialysis tubing for 3–4 days at 40°C to remove salts and methacrylic acids. The solution was lyophilized for 7 days and was subsequently stored at −80°C.

2.3 Scanning electron microscope

The structure of the GelMA hydrogel was analyzed using a scanning electron microscope (SEM). The swollen hydrogels were frozen and were subsequently lyophilized. The lyophilized samples were cut and their cross-sections were coated with platinum using a turbo sputter coater (EMITECH, K575X). SEM images were acquired at a high voltage of 20 kV. The quantifications of the porosity and aspect ratio were analyzed by Image J software.

2.4 Culture of NSCs and tumors

The human NSCs (ReN VM cell line) were cultured on a laminin-coated culture flask with DMEM: Nutrient Mixture F-12 (DMEM:F12), 2% B27 supplement, 1% L-glutamine, 10 μg/mL gentamycin (Invitrogen, Auckland, New Zealand), and 10 units/mL heparin (Sigma, MO, USA) in an incubator (5% CO_2, 37°C). Accutase was used to detach the cells adhered to a tissue culture flask. We also cultured human breast carcinoma cell lines (MCF7). The cells were cultured with DMEM with 10% fetal bovine serum and 1% penicillin–streptomycin.

2.5 Loading of GelMA hydrogels and cell-encapsulated collagen gels

Lyophilized 25 w/v% GelMA hydrogels were mixed into PBS and 0.5% w/v 2-hydroxy-1-(4-(hydroxyethoxy)phenyl)-2-methyl-1-propanone (Irgacure 2959, CIBA Chemicals) as a photo-initiator at 80°C. Eight microliters of GelMA hydrogel solution injected into the inlet of microchamber c in the 3D microfluidic culture device (Fig. 1A) and it was photo-crosslinked by an UV light (360–480 nm wavelength) for 20 s. To culture cells in a 3D manner, 2×10^6 cells/mL suspension of NSCs and tumors was encapsulated within 2 mg/mL collagen type I gels on an ice. Six microliters of cell-encapsulated collagen gels injected into the inlets of microchambers b and d in the 3D microfluidic culture device (Fig. 1A). The cells were incubated at 37°C for 30 min.

2.6 Immunocytochemistry

The cells were fixed with 4% paraformaldehyde for 15 min at room temperature after culturing for 6 days in the GelMA hydrogel-based 3D microfluidic culture device. After washing with PBS, the cells were permeabilized by 1% triton X-100 in PBS for 30 min at room temperature and were subsequently blocked by 1% BSA(Sigma) for 1 h. The cells were immunostained by the primary antibody (anti-Neuronal Class III β-Tubulin (Tuj1; Stem Cell Technology, Canada) and anti-MAP2 (Millipore, Germany)) overnight. They were subsequently incubated with secondary antibody Alexa Fluor 488 goat anti-mouse IgG, (Invitrogen, USA) and Alexa fluor 594 phalloidin (Invitrogen) for 6 h at room temperature. The cell nuclei were also stained by DAPI (0.1 μg/mL) for 30 min at room temperature.

3 Results and discussion

3.1 Fabrication of GelMA hydrogel-based 3D microfluidic culture device

We developed the photo-crosslinkable GelMA hydrogel-based 3D microfluidic culture device (Fig. 1). The GelMA hydrogel-based 3D microfluidic device fabricated by two-step photolithography process was consisted of five microchambers (chambers a–e) and four bridge microchannels (Fig. 1A). The five microchambers (250 μm thickness) were connected with microgrooved four bridge channels (40 μm thickness; Fig. 1B). We made 250-μm thick microchambers for polymerization of GelMA hydrogels and cell-encapsulated collagen type I gels. We also used 40-μm thick microgrooved bridge channels to increase the fluidic resistance. GelMA hydrogels were photo-crosslinked through a mask film via a UV light in the microchamber c. After photo-polymerization of GelMA hydrogels, the inlets and outlets of the microchamber c were sealed by hybrid sealing tapes, showing that it prevented evaporation from solutions in inlets and outlets of microchamber c. We used the photo-crosslinked GelMA hydrogel in the microchamber c as a physical barrier to inhibit the molecular diffusion across bridge microchannels. The cell-encapsulated collagen type I gels loaded into microchambers b and d. The cells were only cultured inside collagen gels in the microchambers because photo-crosslinkable GelMA hydrogels might damage the cells due to UV light-mediated polymerization process. The biocompatibility of GelMA hydrogels was better than other photo-crosslinkable hydrogels (e.g. polyethylene glycol) because GelMA hydrogels contained gelatin generated by partial hydrolysis of collagen. Neurons and glia cells have previously been cultured in the multicompartment microfluidic devices [28]. Axons of central nervous system neurons were isolated in six satellite multicompartment microchannels. It observed the effect of axon layers on astrocytes and oligodendrocyte progenitor cells, showing that axon layers were disrupted by astrocytes, because axons grew

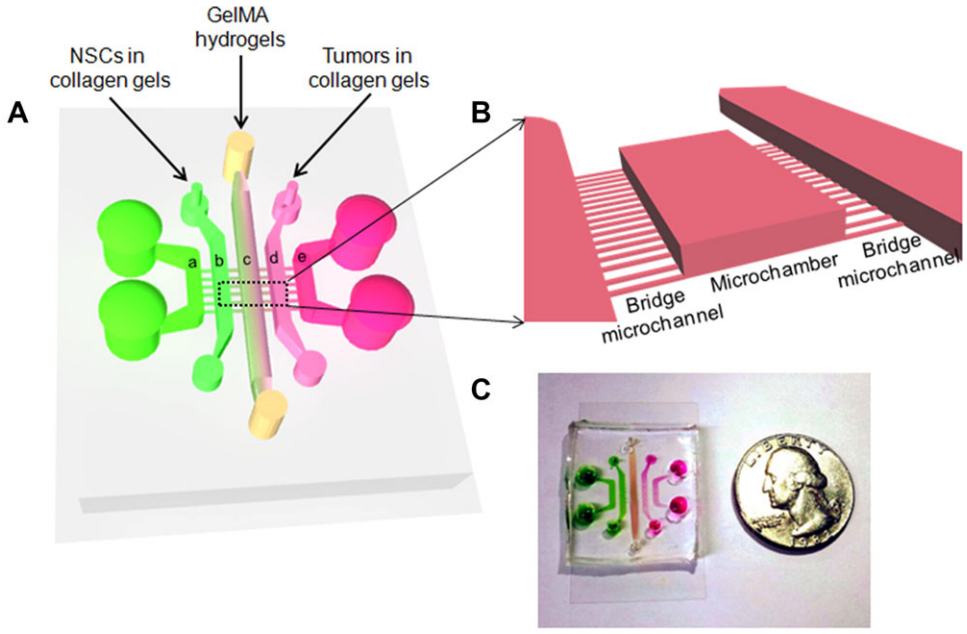

Figure 1. Photo-crosslinkable hydrogel-based 3D microfluidic culture device. (A) Schematic drawing of the photo-crosslinkable hydrogel-based 3D microfluidic device containing five microchambers and four bridge microchannels. (B) Schematic of cross-sectional the photo-crosslinkable hydrogel-based 3D microfluidic culture device. (C) Photograph of photo-crosslinkable hydrogel-based 3D microfluidic culture device.

above astrocytes and astrocytes pushed away axons. In contrast, the mature myelin proteins were highly expressed in oligodendrocyte progenitor cells. Therefore, this multicompartment microfluidic culture device is of great benefit for regulating axon–glia interactions and high-throughput drug screenings. Neurons and astrocytes have also been cultured in the microfluidic device to mimic amyotrophic lateral sclerosis disease [29]. Neural cells were cultured with infected astrocytes without direct cell–cell contacts in the microfluidic device that could generate cell–cell metabolic gradients. It demonstrated that the density of neurons cultured with infected astrocytes was largely decreased. Glutamate gradients were generated in the microfluidic device, showing that moderate treatment of glutamate did not affect death of neurons. Although these previous microfluidic culture devices investigated neuron–glia cell interactions, the previous studies did not consider the photo-crosslinkable hydrogel-based 3D microfluidic device for culture of NSCs and tumors.

3.2 Effects of GelMA hydrogel concentrations on the porosity and diffusion

We observed the effect of GelMA hydrogel concentrations on the porosity, showing that the pore size was inversely proportional to GelMA hydrogel concentrations (Fig. 2). SEM images indicated that the porosity of 25 w/v% GelMA hydrogels showed uniform sizes and shapes compared to 5 w/v% GelMA hydrogels (Fig. 2A–C). It revealed that the pore size of 5 w/v% GelMA hydrogels was 34 μm, whereas 25 w/v% GelMA hydrogels showed 4 μm porosity (Fig. 3A). We observed that the porosity of 25 w/v% GelMA hydrogels showed circular shapes (aspect ratio = 1), whereas 5 w/v% GelMA hydrogels were elliptical shapes (aspect ratio = 1.9, Fig. 3B). Furthermore, we investigated the effect of GelMA hydrogel concentrations on the molecular diffusion (Fig. 4). The fluorescein isothiocyanate (FITC)-dextran (20 kDa) loaded into the microchamber b and 5–25 w/v% GelMA hydrogels were photo-patterned in the microchamber c. It showed that 25 w/v% GelMA hydrogels inhibited the molecular diffusion for 6 days, suggesting 25 w/v% GelMA hydrogel would be used as a physical barrier in the microchamber c (Fig. 4B). In contrast, FITC-dextran solutions were diffused across 5–15 w/v% GelMA hydrogel-based microfluidic chambers. Interestingly, FITC-dextran solutions in the microchamber b largely diffused into the microchamber d at 1 day, when 5 w/v% GelMA hydrogels (34 μm porosity) were used in the microchamber c. In contrast, FITC-dextran solutions in chamber b were not diffused into the microchamber d for

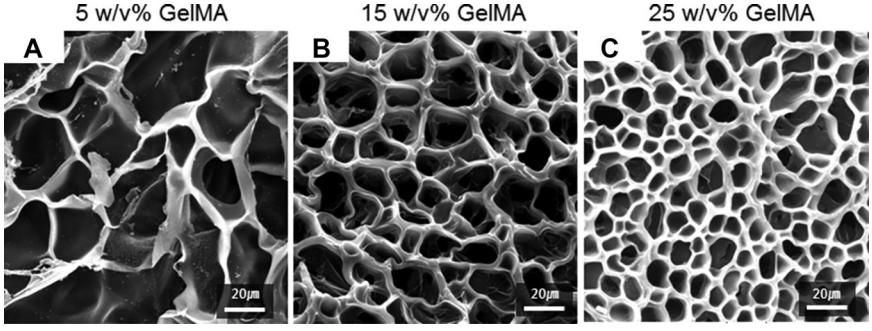

Figure 2. SEM images of (A) 5 w/v%, (B) 15 w/v%, and (C) 25 w/v% photo-crosslinkable GelMA hydrogels. Scale bars are 20 μm.

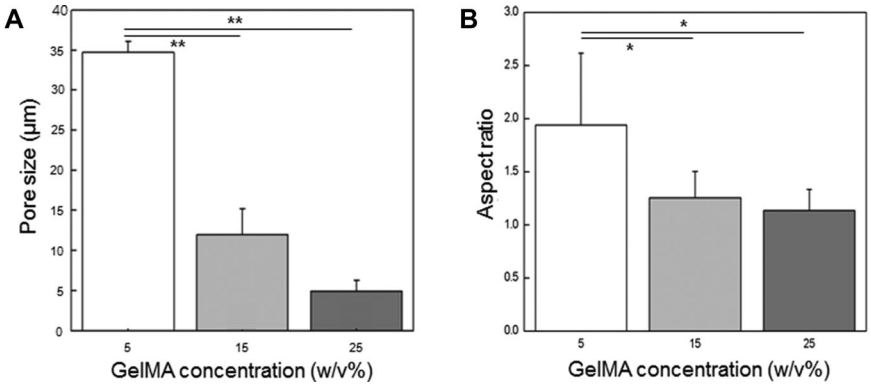

Figure 3. Effect of GelMA hydrogel concentrations (5–25 w/v%) on (A) pore size and (B) aspect ratio. The aspect ratio means the ratio of the length of pores divided by width of pores (*$p < 0.05$, **$p < 0.01$).

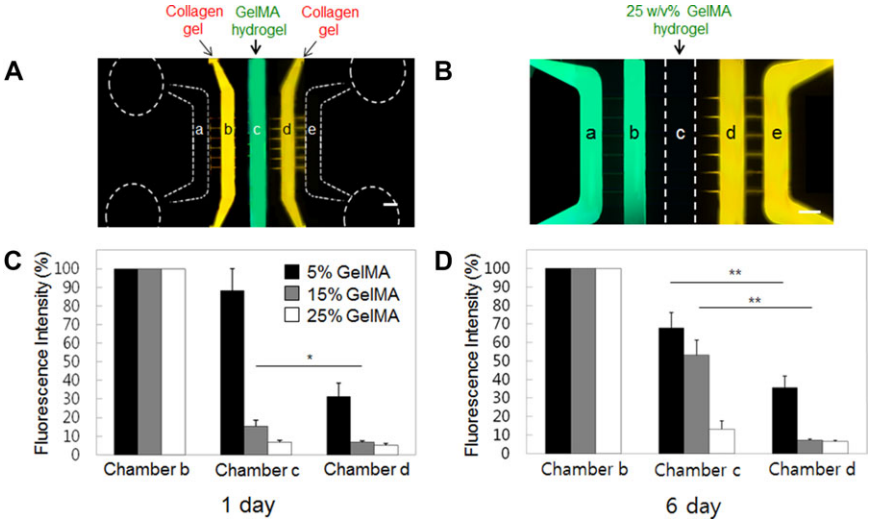

Figure 4. Analysis of the diffusion across the photo-crosslinkable GelMA hydrogel-loaded 3D microfluidic culture device. (A) The fluorescent image showing the GelMA hydrogel-loaded microchamber c and collagen type I gel-loadedmicro chambers b and d. (B) The fluorescent image indicating the green fluorescent dye-loaded microchambers a and b, 25 w/v% GelMA hydrogel-loaded microchamber c, and red fluorescent dye-loaded microchambers d and e. Analysis of the chemical diffusion across the GelMA hydrogel-loaded microchamber c at (C) 1 day and (D) 6 days (*$p < 0.05$, **$p < 0.01$). The FITC-dextran (20 kDa) solution is loaded into microchamber b. The fluorescent molecules are diffused from microchamber b to chamber d. Scale bars are 1 mm.

6 days, when 25 w/v% GelMA hydrogels (4 μm porosity) were employed in the microchamber c. As a result, we demonstrated that 4 μm porosity of 25 w/v% GelMA hydrogels and 210 μm thickness gaps between microchambers (250 μm in thickness) and bridge microchannels (40 μm in thickness) inhibited the molecular diffusion. We also modified the design of our microfluidic device (Fig. 5). Square-shaped four microchambers (250 μm in thickness) were connected by two bridge microchannels (40 μm in thickness). 5–25 w/v% GelMA hydrogels loaded into two bridge microchannels to confirm the effect of GelMA hydrogel concentrations on chemical diffusion. We performed chemical diffusion experiments for 6 days in the microfluidic device. Similar to diffusion results (Fig. 4) of the previous design (Fig. 1), 25 w/v% GelMA hydrogels in bridge microchannels inhibited the chemical diffusion from square-shaped microchambers, suggesting that four different cell types would be cultured inside each square-shaped microchamber. The effect of GelMA hydrogel concentrations on swelling degree has previously been investigated [26]. It demonstrated that the mass swelling ratio was inversely proportional to GelMA hydrogel concentrations, indicating that the swelling ratio at 15 w/v% GelMA hydrogels was 50% decreased compared to 5 w/v% GelMA hydrogels. It suggested that high concentrations of GelMA hydrogels might prevent molecular diffusions. GelMA hydrogels have previously been used in the bilayer microfluidic device to regulate the cell–cell interactions [30]. The valvular endothelial cells were cultured on the porous membrane, while valvular interstitial cells encapsulated within the GelMA hydrogel were cultured below porous membrane. GelMA hydrogels showed higher mechanical stability and physiologically relevant elastic moduli. It demonstrated the effect of shear stress on paracrine interactions between valvular interstitial cells and valvular endothelial cells. However, these previous studies did not consider the GelMA hydrogel as a physical barrier in the microfluidic device.

3.3 Culture of NSCs and tumors in the 3D microfluidic device

Cultures of NSCs and tumors are of great interest in applications for regenerative tissue constructs. NSCs and tumors were cultured for 6 days on a 2D surface and 3D collagen gel (Fig. 6). The confocal microscopy images showed that the morphologies of NSCs and tumors cultured within 3D collagen gels were different compared to 2D surfaces. We observed that NSCs and tumors cultured on 2D surfaces were

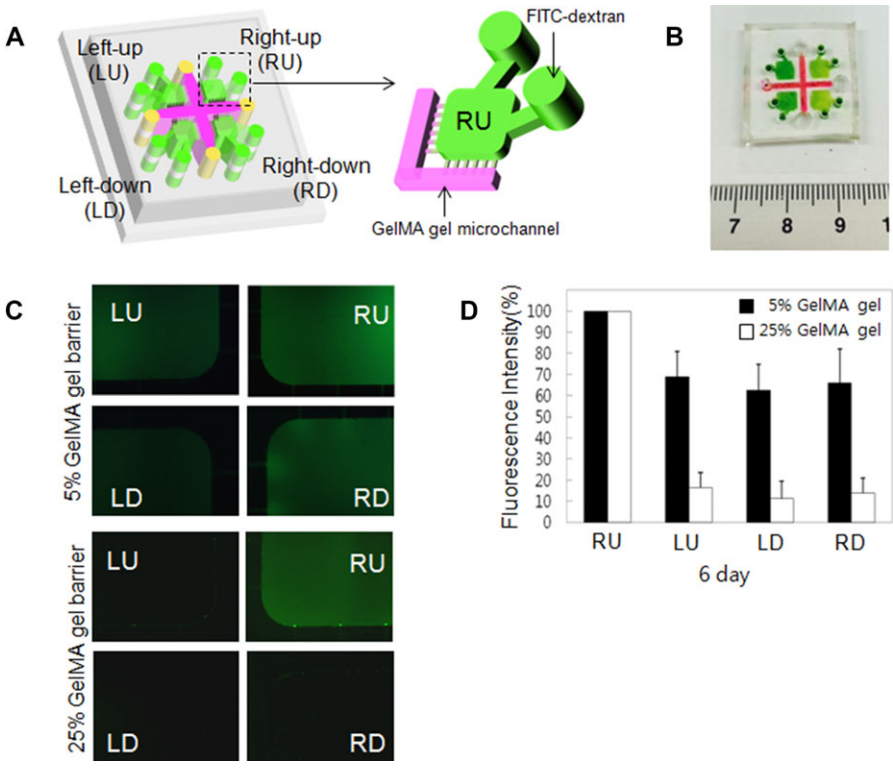

Figure 5. The modified design of the 3D microfluidic device. (A) Schematic drawing of the modified design of the 3D microfluidic device containing four square-shaped microchambers (Left-up (LU), Right-up (RU), Left-down (LD), and Right-Down (RD)) and 5–25 w/v% GelMA hydrogel-loaded eight bridge microchannels. (B) Photograph of the modified design of the 3D microfluidic device. (C) Fluorescent images of the chemical diffusion. (D) Analysis of the chemical diffusion across 5 and 25 w/v% GelMA hydrogel-loaded bridge microchannels at sixth day. The FITC-dextran (20 kDa) was only loaded into RU microchamber and chemical diffusion was analyzed in LU, LD, and RD microchambers.

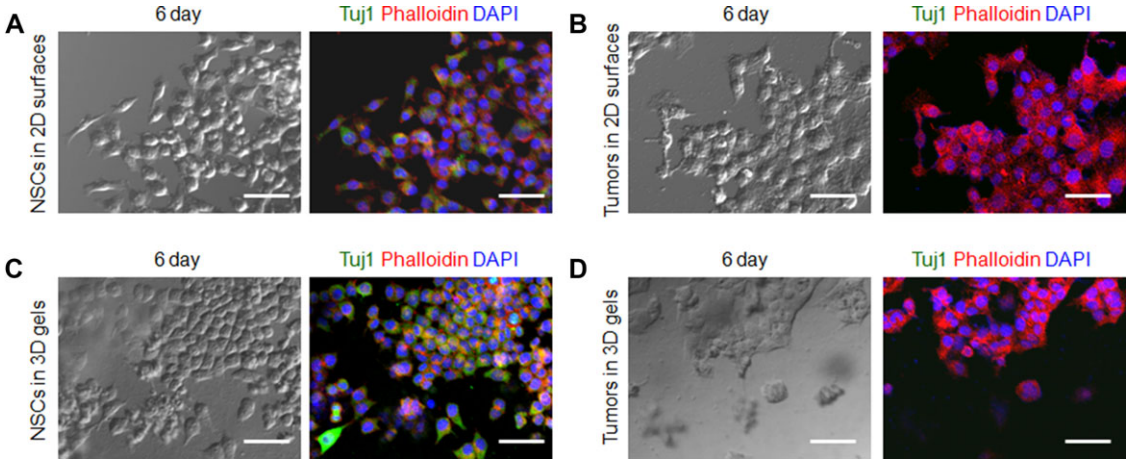

Figure 6. NSCs and tumors cultured in 2D surfaces and 3D collagen gels. (A) Confocal microscopy image of NSC-derived neurons cultured for 6 days on 2D surfaces. (B) Confocal microscopy image of tumors cultured for 6 days on 2D surfaces. (C) Confocal microscopy image of neuronal differentiation from NSCs cultured for 6 days in 3D collagen gels. (D) Confocal microscopy image of tumors cultured for 6 days in 3D collagen gels. Scale bars are 50 μm.

relatively polarized (Fig. 6A), whereas the shape of NSCs and tumors cultured in 3D collagen gels were round (Fig. 6C and D). In parallel, we investigated the effect of 3D collagen gels on the behavior of NSCs and tumors in the 3D microfluidic culture device as shown in Figs. 1 and 7. NSCs and tumors encapsulated with collagen type I gels were loaded into the microchambers b and d, respectively. 25 w/v% GelMA hydrogels loaded into the microchamber c to prevent the medium diffusion from bridge microchannels. The confocal microscopy images represented that Tuj1- or MAP2-positive neurons were highly expressed in the collagen gel-loaded microchamber b (Fig. 7A, C, E), whereas phalloidin-positive tumors were cultured in the collagen gel-loaded microchamber d (Fig. 7B, D, F). The immunocytochemistry analysis showed that 53–75% NSCs differentiated into Tuj1- or MAP2-positive neuronal cells in the hydrogel-based 3D microfluidic culture device (Fig. 7G). It has been known that stem cell differentiation could be affected by the fluidic flow [31]. However, we used 25 w/v% GelMA hydrogel as a physical barrier to prevent chemical diffusion from microchambers. Thus, the effect of the interstitial fluid on NSC differentiation might be negligible in the microfluidic device. The interaction between breast cancer cells and NSCs has previously been investigated for studying the tumor therapy. For instance,

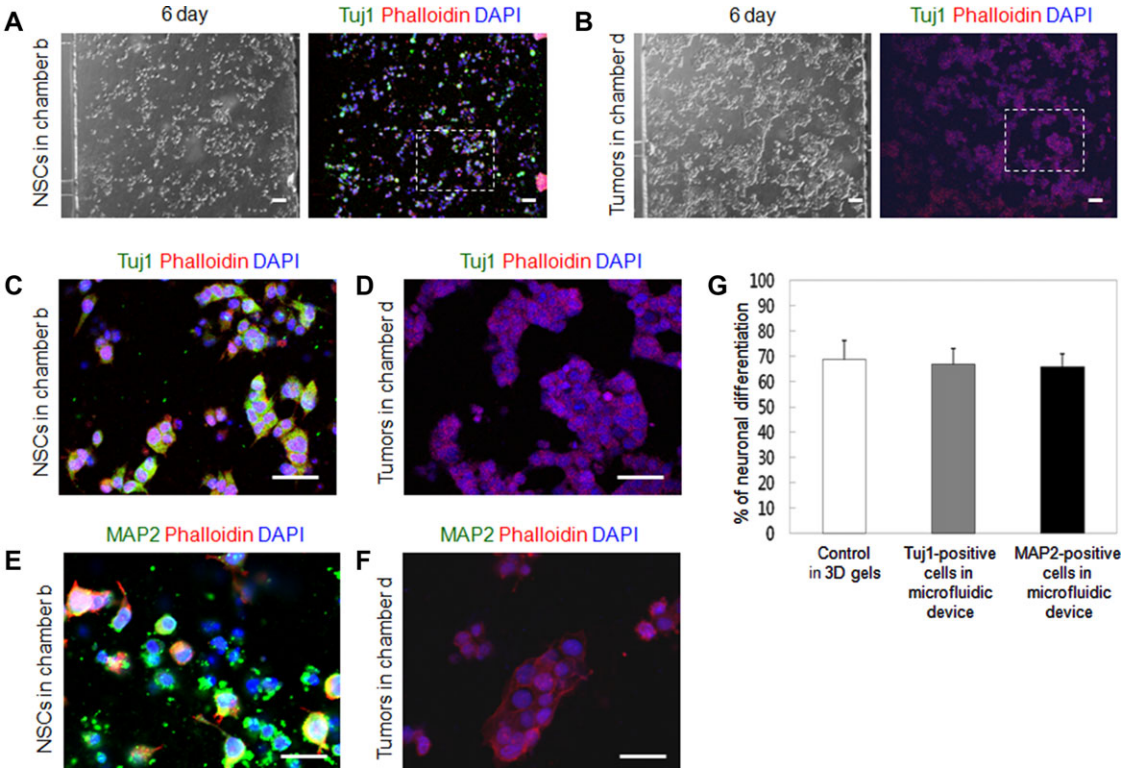

Figure 7. NSCs and tumors in the hydrogel-based 3D microfluidic culture device of Fig. 1. (A) Confocal microscopy image of neuronal differentiation from NSCs cultured for 6 days in the hydrogel-based 3D microfluidic culture device. (B) Confocal microscopy image of tumors cultured for 6 days in the hydrogel-based 3D microfluidic culture device. (C) High-magnification confocal microscopy image of the white-dotted box in (A). (D) High-magnification confocal microscopy image of the white-dotted box in (B). (E) High-magnification confocal microscopy image of MAP-2-positive neuronal cells in cultured in microchamber b. (F) High-magnification confocal microscopy image of phalloidin-positive tumor cells in cultured in microchamber d. (G) Analysis of NSC-derived neuronal differentiation in the photo-crosslinkable hydrogel-based 3D microfluidic culture device. Scale bars are 50 μm.

the human-induced pluripotent stem cell-derived NSCs have used for gene therapy applications of breast cancer cells [32, 33]. NSCs were generated from human-induced pluripotent stem cells. For the tumor gene therapy, the human-induced pluripotent stem cell-derived NSCs were transduced by a baculoviral vector with kinase suicide genes. It demonstrated that NSCs migrated into the mouse breast tumors and inhibited the metastasis of breast tumors. Therefore, our 3D microfluidic culture device could also be useful for regulating the behaviors of NSCs and tumors.

4 Concluding remarks

We developed the photo-crosslinkable hydrogel-based 3D microfluidic device to culture NSCs and tumors. We observed the effects of photo-crosslinkable GelMA hydrogel concentrations on the porosity, indicating 25 w/v% GelMA hydrogels showed the circular-shaped porosity with 4 μm in diameter. We successfully demonstrated that 53–75% NSCs differentiated into Tuj1- or MAP2-positive neurons, while tumors were cultured for 6 days in the 3D microfluidic device, because 25 w/v% GelMA hydrogel was used as a physical barrier to inhibit the molecular diffusion. Therefore, this photo-crosslinkable hydrogel-based 3D microfluidic culture device could be a potentially powerful tool for regenerative tissue engineering applications.

This research was supported by BioNano Health-Guard Research Center funded by the Ministry of Science, ICT & Future Planning (MSIP) of Korea as Global Frontier Project (grant number H-GUARD_2014M3A6B2060503), Republic of Korea. This work was also supported by Leading Foreign Research Institute Recruitment Program through the National Research Foundation of Korea (NRF) funded by the Ministry of Science, ICT & Future Planning (MSIP) (grant number 2013K1A4A3055268). This work was also supported by a grant of the Korea Health Technology R&D Project through the Korea Health Industry Development Institute, funded by the Ministry of Health & Welfare, Republic of Korea (Grant number HI14C3347).

The authors have declared no conflict of interest.

5 References

[1] Lie, D. C., Song, H., Colamarino, S. A., Ming, G. L., Gage, F. H., *Annu. Rev.Pharmacol. Toxicol.* 2004, *44*, 399–421.

[2] Singec, I., Jandial, R., Crain, A., Nikkhah, G., Snyder, E. Y., *Annu. Rev. Med.* 2007, *58*, 313–328.

[3] Temple, S., *Nature* 2001, *414*, 112–117.

[4] Ma, W., Fitzgerald, W., Liu, Q. Y., O'Shaughnessy, T. J., Maric, D., Lin, H. J., Alkon, D. L., Barker, J. L., *Exp. Neurol.* 2004, *190*, 276–288.

[5] Brannvall, K., Bergman, K., Wallenquist, U., Svahn, S., Bowden, T., Hilborn, J., Forsberg-Nilsson, K., *J. Neurosci. Res.* 2007, *85*, 2138–2146.

[6] Fisher, O. Z., Khademhosseini, A., Langer, R., Peppas, N. A., *Acc. Chem. Res.* 2010, *43*, 419–428.

[7] Lee, K. Y., Mooney, D. J., *Chem. Rev.* 2001, *101*, 1869–1879.

[8] Wan, C. Y., Frydrych, M., Chen, B. Q., *Soft Matter* 2011, *7*, 6159–6166.

[9] De Paepe, I., Declercq, H., Cornelissen, M., Schacht, E., *Polym. Int.* 2002, *51*, 867–870.

[10] Shin, S. R., Bae, H., Cha, J. M., Mun, J. Y., Chen, Y. C., Tekin, H., Shin, H., Farshchi, S., Dokmeci, M. R., Tang, S., Khademhosseini, A., *ACS Nano* 2012, *6*, 362–372.

[11] Leipzig, N. D., Wylie, R. G., Kim, H., Shoichet, M. S., *Biomaterials* 2011, *32*, 57–64.

[12] Nuttelman, C. R., Tripodi, M. C., Anseth, K. S., *J. Biomed. Mater. Res. A* 2004, *68*, 773–782.

[13] DeForest, C. A., Polizzotti, B. D., Anseth, K. S., *Nat. Mater.* 2009, *8*, 659–664.

[14] Li, H., Wijekoon, A., Leipzig, N. D., *PLoS One* 2012, *7*, e48824.

[15] Seidlits, S. K., Khaing, Z. Z., Petersen, R. R., Nickels, J. D., Vanscoy, J. E., *Biomaterials* 2010, *31*, 3930–3940.

[16] Chandler, E. M., Berglund, C. M., Lee, J. S., Polacheck, W. J., Gleghorn, J.P., Kirby, B. J., Fischbach, C., *Biotechnol. Bioeng.* 2011, *108*, 1683–1692.

[17] Morrison, S. J., Spradling, A. C., *Cell* 2008, *132*, 598–611.

[18] Chung, B. G., Flanagan, L. A., Rhee, S. W., Schwartz, P. H., Lee, A. P., Monuki, E. S., Jeon, N. L., *Lab Chip* 2005, *5*, 401–406.

[19] Lee, J. M., Kim, J. E., Borana, J., Chung, B. H., Chung, B. G., *Electrophoresis* 2013, *34*, 1931–1938.

[20] Han, S., Yang, K., Shin, Y., Lee, J. S., Kamm, R. D., Chung, S., Cho, S. W., *Lab Chip* 2012, *12*, 2305–2308.

[21] Lee, J. M., Kim, J. E., Kang, E., Lee, S. H., Chung, B. G., *Electrophoresis* 2011, *32*, 3133–3137.

[22] Patra, B., Chen, Y. H., Peng, C. C., Lin, S. C., Lee, C. H., Tung, Y. C., *Biomicrofluidics* 2013, *7*, 54114.

[23] Shin, H. S., Kim, H. J., Min, S. K., Kim, S. H., Lee, B. M., Jeon, N. L., *Biotechnol. Lett.* 2010, *32*, 1063–1070.

[24] Torisawa, Y. S., Mosadegh, B., Luker, G. D., Morell, M., O'Shea, K. S., Takayama, S., *Integr. Biol.* 2009, *1*, 649–654.

[25] Taylor, A. M., Rhee, S. W., Tu, C. H., Cribbs, D. H., Cotman, C. W., Jeon, N. L., *Langmuir* 2003, *19*, 1551–1556.

[26] Nichol, J. W., Koshy, S. T., Bae, H., Hwang, C. M., Yamanlar, S., Khademhosseini, A., *Biomaterials* 2010, *31*, 5536–5544.

[27] Van Den Bulcke, Al., Bogdanov, B., DeRooze, N., Schacht, E. H., Cornelissen, M., Berghmans, H., *Biomacromolecules* 2000, *1*, 31–38.

[28] Park, J., Koito, H., Li, J., Han, A., *Lab Chip* 2012, *12*, 3296–3304.

[29] Kunze, A., Lengacher, S., Dirren, E., Aebischer, P., Magistretti, P. J., Renaud, P., *Integr. Biol.* 2013, *5*, 964–975.

[30] Chen, M. B., Srigunapalan, S., Wheeler, A. R., Simmons, C. A., *Lab Chip* 2013, *13*, 2591–2598.

[31] Blagovic, K., Kim, L.Y., Voldman, J., *PLoS One* 2011, *6*, e22892.

[32] Shang, X., Marchioni, F., Sipes, N., Evelyn, C. R., Jerabek-Willemsen, M., Duhr, S., Seibel, W., Wortman, M., Zheng, Y., *Chem. Biol.* 2012, *19*, 699–710.

[33] Yang, J., Lam, D. H., Goh, S. S., Lee, E. X., Zhao, Y., Tay, F. C., Chen, C., Du, S., Balasundaram, G., Shahbazi, M., Tham, C. K., Ng, W. H., Toh, H. C., Wang, S., *Stem Cells* 2012, *30*, 1021–1029.

